VANADIUM REDOX FLOW BATTERY MODELLING AND PV SELF-CONSUMPTION MANAGEMENT STRATEGY OPTIMIZATION

Ana Foles, Luís Fialho, Manuel Collares-Pereira, Pedro Horta
Renewable Energies Chair, University of Évora
Plataforma de Ensaio de Concentradores Solares, Herdade da Mitra - Valverde, 7000-083 Nossa Senhora da Tourega, Évora, Portugal

ABSTRACT: This work aims to maximize the photovoltaic solar electricity's self-consumption, through the development and validation of an equivalent electric model of a vanadium redox flow battery and its implementation in an energy management strategy. The first phase of the work presents the modelling of the 5.0 kW/60 kWh VRFB integrated in a solar photovoltaic microgrid - 3.5 kWp monocrystalline plus 3.2 kWp polycrystalline technology - at the University of Évora. The model is based in the equivalent electric circuit model built upon the consulted bibliographic references allowing to calculate the battery parameters on the desired power. It considers the auxiliary power consumption and operational parameters and despite its simplicity attains for a good match with experimental results. Upon its validation, the model is further enhanced as to better describe the VRFB real response in its regular operating conditions. Assessment of the enhanced model is based on key performance indicators such as self-consumption rate, rate of battery usage or electric grid independence. In this work an approach to best fit the battery modelling and simultaneously the energy management strategy for a PV+VRFB system is presented, based on actual operating conditions and on a prescribed EMS goal.
Keywords: Characterisation, Storage, Strategy

1 INTRODUCTION

In 2017 the solar photovoltaic (PV) reached a total installed capacity 98 GW. For 2019 the PV stood for 3% of the total global power generation mix, with a 2050 forecast of 23% [1]. Its relevance is being noticed in the countries' national plans worldwide. Increased PV capacity in the power generation system, combined with higher capacity of other low dispatchability renewable electricity sources such as wind, raise the importance of electricity storage as the power distribution system requires a due management of dispatchability. Despite its importance, battery storage technologies still face challenges as turnkey solutions.
Fostering the study and demonstration of different electricity storage technologies, and in the framework of the project PVCROPS 2012-2015 [308468], the Renewable Energies Chair of the University of Évora (CER-UÉvora) has installed and fully integrated a Vanadium Redox Flow Battery (VRFB), 5kW/60kWh, manufactured by REDT company [2] in a microgrid – Figure 1 and 2. This microgrid is currently exclusively devoted for its testing and systems operation study, and integration with the building at real scale.

Figure 1: VRFB by manufacturer REDT, 60/5 kWh/kW, installed in the University of Évora.

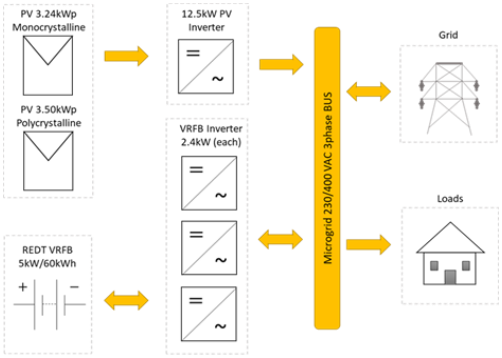

Figure 2: VRFB microgrid.

This microgrid is equipped with a PV system with 3.5 kW_p of polycrystalline technology and 3.2 kW_p of monocrystalline technology – Figure 3 –, precision monitoring equipment and the control system.
The RFBs are a promising choice for stationary electricity storage in electric grids, regarding power quality and energy management services:

- Power rating depends on stack sizing and stored-energy rating depends on the volume of the tanks. The decoupling of power rating and storage capacity is a competitive advantage of RFBs towards other battery technologies;
- Its response is usually fast, and it is associated to longer lifetimes and low maintenance requirements. It stores energy in two electrolytic solutions with two different redox couples.
- The stack, the energy conversion unit, is made of several cells, forming two electrodes separated by a proton selective membrane. The electrolyte is pumped from the tanks to the stack, where the half-electrochemical reactions occur. [3].

The present RFBs have different chemistries: bromine-polysulphide, hydrogen-bromine, magnesium-vanadium, vanadium-bromine, vanadium-cerium,

vanadium-oxygen, vanadium polyhalide, vanadium-vanadium, zinc-bromine, zinc-cerium. Although all these configurations, the vanadium-vanadium chemistry is the most mature so far. Introduced in the 1970s and already marketed, there are still some aspects of its operation to explore and improve. The VRFB has the vanadium element in four oxidation states mixed in an aqueous solution of sulfuric acid:

Negative electrode	Positive electrode
▪ V^{2+} (bivalent)	▪ VO^{2+} (tetravalent)
▪ V^{3+} (trivalent)	▪ $VO_2{}^{+}$ (pentavalent)

Being the electrochemical reactions the following:

- In charge operation:

Negative electrode: $V^{3+} + e^- \rightarrow V^{2+}$

Positive electrode: $VO^{2+} + H_2O \rightarrow VO_2{}^{+} + 2H^+ + e^-$

- In discharge operation:

Negative electrode: $V^{2+} \rightarrow V^{3+} + e^-$

Positive electrode: $VO_2{}^{+} + 2H^+ + e^- \rightarrow VO^{2+} + H_2O$

The electrodes are a highly porous carbon/graphite felts, properly treated to improve its hydrophilic capacity, and achieve catalytic effects. This bipolar plate (which exists between each cell), creates the electrical connection between the two opposite poles.

Figure 3: University of Évora's PV installation.

The VRFB's stack is a dynamic system, and its performance depends on multiple effects: electrochemical, fluid dynamics, electric and thermal. To obtain the system description, non-linear equations are used, as follows [3]:

- Butler-Volmer equation – Describes electrochemical kinetics and activation overpotentials, as a function of the current density;
- Nernst-Plank equation – Describe the mass transport and ions in the electrodes;
- Vogel-Tammam-Fulcher equation – Considers the ions transport in the membrane;
- *Lattice-Boltzmann model* – Considers the non-linear superdiffusive behaviour of the ions in mesoscale, in anisotropic porous media.

These models are the basis of the multiphysics models which are currently used to describe the VRFB [4]. The level of detail of the model determines the computational resource and processing time to simulate the battery operation [5].

A detailed electric equivalent model considers the loss in the membrane, electrochemical activation in the positive and negative electrodes and the mass flow in the electrodes as resistances, and capacitors representing the double layer effects on the reaction surfaces inside the electrodes. Controlled current sources are used to represent the species crossover between the two electrodes (diffusion e electroosmotic drag), the energy absorption of pumps in circulation as controlled current sources, and an equivalent shunt resistance to account the shunt currents in the solutions. The aim of this work is to use a model which represents the battery system with adequate precision and that considers the interfaces with the power converters, the battery BMS, and the active components (pumps and valves). To model these components, simpler models are used, such as equivalent circuits that have reduced complexity and satisfying results. In a more simplified approach, it can be concluded that the losses of electrochemical activation are much lower than the ohmic losses of the membrane at full load. Concentration losses are important when the rated current density is exceeded.

Some VRFB models are found in literature, depending on the desired degree of detail. A very detailed modelling review is made by Chakrabarti et al [6], although a simpler model is needed for real world fast computing applications. Chahwan et al. [7] investigated a simple model application, evaluating the fitting for one charge and discharge, achieving satisfactory results. Similar models are the ones developed by D'Agostino et al [5], Nguyen et al [8] and Qiu et al [9], with interesting results on field validations. With an extended Kalman filter, Mohamed [10] explored a model for a unit cell. Wei et al [11] developed an online adaptative model of a VRFB to better reproduce its dynamics. Bhattacharjee et al [12] studied a general electrical model, and also an online SOC estimation. The reviewed models are important benchmarks for the VRFB modelling and were the starting point of this work, giving more emphasis to operational and controlling real-time aspects, in conjunction with the modelling. Considering the aim of developing a model to integrate in an energy management strategy (EMS) for the microgrid as a whole, a compromise between accuracy, simplicity and computational effort possible was assumed in for the model herein presented, implemented in MATLAB [13], and further compared against real data for charge and discharge. The application of the developed model to the EMS is evaluated and discussed, and the strategy merit factors are investigated.

2 BATTERY CHARACTERIZATION

The manufacturer REDT made available the data presented in Table I, which is very important information, but not enough to an accurate model. To achieve a robust model, additional details should be used to the battery general characterization. Aiming at gathering data and sensibility to real scale / real-time operation performance, the battery was subjected to characterization tests: six successive full cycles of charge and discharge under reference operating conditions, ranging the state of charge (SOC) from 5% to 90%. To achieve this characterization a dedicated control was developed and implemented in LabVIEW, communicating and registering all the microgrid data

with a timestep of 4-5 seconds. This program is followed by precision monitoring to compare the obtained data and correct possible errors in real-time. It registers active and reactive power, voltage, current and many other variables, along the power exchanged with the microgrid.
VRFB is composed by a reference cell, Figure 4, which is hydraulically connected in parallel with the stack, subjected to the same electrolyte flux, without being subjected to charge or discharge, with the aim of making direct real-time voltage measurements. This voltage represents the battery real voltage, since it is only affected by the electrolyte real oxidation state. Through this measurement it is possible to know the real SOC of the battery, through a manufacturer given relation SOC-one cell voltage.

Table I: REDT available data.

Manufacturer technical specifications	
Rated energy capacity (kWh)	60
Number of cells in the stack	40
Operating voltage range (V)	Up to 65
Volume (m^3)	1.8 (each tank)
Depth of discharge (%)	95
Lifetime (cycles)	+10000

Figure 4: Stack of the VRFB and its reference cell.

Battery characterization test data was analyzed, and average results are presented in Table II.

Table II: Experimental obtained parameters.

VRFB performance	**Results**
Total capacity (kWh)	86.3 ± 2.30
Useful maximum capacity (kWh)	66.5 ± 4.26
Energy density (Wh/L)	17.5 ± 4.26
Fastest charge (h)	51h41
Fastest discharge (h)	26h54
Charge/discharge efficiency	77.1 ± 3.36
Maximum power (kW)	5.0
Response time	Seconds (s)
Cell voltage operating range (V)	1.249-1.513
Typical response time	Hours

The values obtained were compared with bibliographic references, [14][15][16][17][18][19], and show consistency.

3 ELECTRICAL VRFB MODEL

To determine the electrical requirements for the power battery management system (BMS), the main effects to be considered are the drop in resistive voltage in the membrane, allowing a simple estimation of the cell voltage, through the Eq. (1) [3]:

$$v_c \cong E(s) - \Delta v_t = E(s) - r_t j \quad (1)$$

The stack losses and battery efficiency are influenced by two main factors: pumps and shunt currents, further discussed. A simplified modelling approach considers cells internal losses and all the battery external losses, since the aim is to detail its electrical behaviour. The model is built upon already existent models of the vanadium redox flow battery, adapting it to the real operation of this battery. In Figure 5 the equivalent electric model is shown.

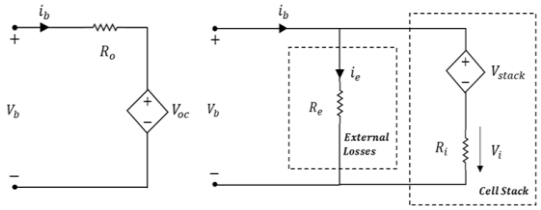

Figure 5 - Equivalent electric model scheme used to describe the VRFB operation.

3.1 Stack Voltage

The battery voltage, V_b , is calculated after Eq. (2):

$$V_b = V_{stack} + i_{stack} R_i \quad (2)$$

Where V_{Stack} is the stack voltage and i_{stack} is the stack current. The stack current is obtained through the application of the Kirchhoff's first law, as Eq. (3) presents:

$$i_{stack} = i_b - i_e \quad (3)$$

Where i_b is the battery current, and i_e the current of the external losses.
The voltage of the stack depends on the SOC, temperature (T, in K), and the number of cells of the stack, n_{cells}. The open circuit voltage is given by the Nernst equation, shown in Eq. (4), which includes the knowing of the electrolyte ions concentration and determines the solution modularity,

$$E = E^0 + \frac{R \times T}{F} \times \ln\left[\frac{C_{VO_2^+}(C_{H^+})^2 C_{V^{2+}}}{C_{VO^{2+}} C_{V^{3+}}}\right] \quad (4)$$

Where, E^0 represents the Gibbs potential, R the universal gas constant (8.314 J/mol.K), T is the temperature in Kelvin, F the Faraday constant (96485 sA/mol). The vanadium ions concentration is given by Eq. (5) and by Eq. (6):

$$C_{V^{2+}} = C_{VO_2^+} = C_V \, SOC \quad (5)$$

$$C_{V^{3+}} = C_{VO^{2+}} = C_V(1 - SOC) \quad (6)$$

The voltage of a single cell of the stack can be approximated to Eq. (7):

$$\frac{V_{Stack}}{n_{cells}} = V_{Soc,50\%} + \frac{R \times T}{F} \times \ln\left[\frac{SOC^2}{(1-SOC)^2}\right] \quad (7)$$

Being the $V_{Soc,50\%}$ the voltage of a single cell at the SOC of 50%. Finally, the total stack voltage is given by Eq. (8),

$$V_{Stack} = n_{cells} \times \left\{ V_{Soc,50\%} + \frac{R \times T}{F} \times \ln\left[\frac{SOC^2}{(1-SOC)^2}\right] \right\} \quad (8)$$

3.2 Resistances

The selected model has a time resolution in the order of microseconds, which is satisfactory for the solar photovoltaic and loads response time as well as our control running time. The cell stack losses are described as one single resistance of Thevenin, R_i, representing the reaction resistive losses. The equivalent resistance is estimated as quasi-constant in processes of charge and discharge, and is represented through Eq. (9),

$$R_i = \sum_{1}^{k} \frac{V_{b,k} - V_{stack,k}}{i_{stack,k}} \quad (9)$$

Being $V_{b,k}$ the battery terminal voltage, $V_{stack,k}$ the stack voltage, $i_{stack,k}$ the stack current, all at instant k. The external losses (pumps) could be achieved using Eq. (10):

$$R_e = \frac{V_b}{i_e} \quad (10)$$

3.3 State of charge

The battery SOC can be calculated through Eq. (11) and Eq. (12).

$$SOC_{t_k} = SOC_t + \Delta SOC_{t_k - t} \quad (11)$$

$$SOC_{t_k} = SOC_t + \int_t^{t_k} \frac{V_{stack}(t) i_s(t)}{E_{Capacity}}\, dt \quad (12)$$

Being the $E_{Capacity}$ (Wh) the total capacity of the battery. This model was compared with experimental data, through the full characterization data obtained of the VRFB real operation, and some adaptation of the model was made to better fit our goal.

4 MODEL ADAPTATIONS AND SIMULATION RESULTS

4.1 Voltage at 50% of SOC and Resistances

Given the manufacturer SOC curve of the VRFB described in [20], the cell reference voltage is 1.400 V, at 50% of SOC, as can be observed with the help of Figure 6. For comparison, the obtained SOC of the battery in the studied interval is calculated through the manufacturer curve, as shown in the work developed in [20].

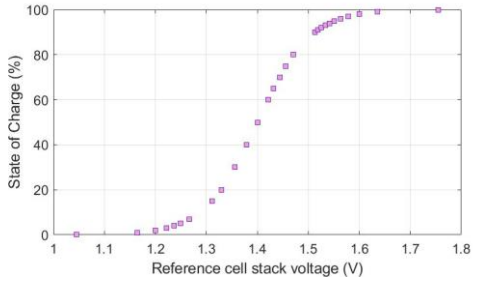

Figure 6: SOC (%) in function of the reference cell stack voltage (V).

After the tests and comparison with the experimental data, the calculation of the resistance after Equation 8 was improved for charge and discharge. An average for each resistance was obtained, with a value of 0.07Ω for charge and 0.20Ω for discharge.

The current needed to power the pumps of the VRFB is considered constant in this work, since its consumption varies very little within the stack voltage of the battery, i.e. the SOC. This value was, on average, 1.8702 A, as can be observed in the following Figure 7, for real charge and discharge data.

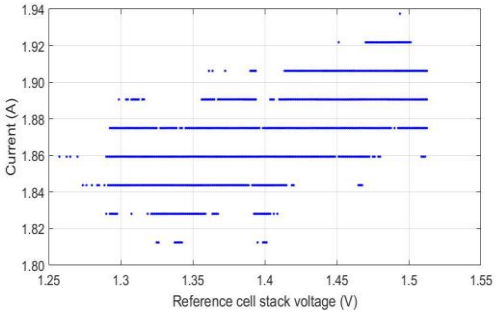

Figure 7: Auxiliar current in function of the reference cell stack voltage.

Besides this adaptation, a sensibility analysis of the obtained results and parameters of the model was made. The relation of the reference cell voltage-SOC had good results, so it does not need further improvements. The V_{soc50} was the value which offered the best fitting.

Unfortunately, the experimental stack current was not measured during the tests, since the sensor was malfunctioning, so this parameter was not evaluated in the scope of the present paper.

4.2 Implementation and validation

The battery was fully characterized within the operational range for the SOC from 5% to 90%, given the operational available power of charge and discharge for that range. The maximum power of either charge or discharge is 5000 W. In the battery room, an air conditioning is working to maintain an ambient temperature of 24ºC. We assume a constant storage temperature of 26ºC. The model input data is shown in Table III. In Figure 8 the obtained values of the voltage stack are given, in conjunction with its relative error.

According to the model application, simulation, and overall control, it is possible to present the obtained parameters of the battery model in Table IV.

Table III: Model input parameters.

Input parameter	Data
Power profile (W)	-
Initial SoC (%)	7.5
Vsoc50 (V)	1.400
Parasitic resistance charge (RPC)	0.05
Parasitic resistance discharge (RPC)	0.07
Losses resistance charge (RCC)	0.04
Losses resistance discharge (RCD)	0.20
Temperature (K)	26+273.15
Number of cells in the stack	40
Faraday constant (As/mol)	96485
Pump DC power (W)	300

Pump AC power (W)	350
Gas constant	8.314

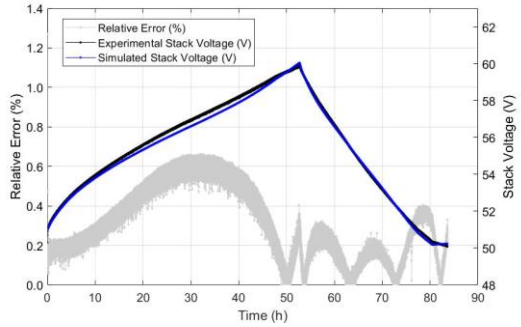

Figure 8: Stack voltage experimental and simulated, and the respective relative error.

Table IV: Obtained model parameters errors.

Parameter	RMSE	Mean relative error
Stack voltage	0.4143 V	0.2991
Voltage terminal	1.3716 V	0.6141
Current terminal	2.8858 A	0.0180

4 EMS – Self-consumption strategy

4.1 EMS

Portugal has in force the Decree-Law 162/2019 (25th October) which gives a very strong emphasis to the renewable energy self-consumption. In that context, we choose to evaluate this model using this EMS, since it is the most suitable strategy for a residential scale. The PV self-consumption maximization with the use of a battery was explored to check the suitability of the application methods in real time operation. A specially devoted LabVIEW programme was developed for this control strategy, with internal implementation of the VRFB model. The user interface is showed in Figure 10.

For this strategy application, real-time data of the PV system over 6 days was tested. The decision to eliminate some parts of the null PV generation was made in order to shorten the time duration of the test in real-time. The load profile is made available by EDP Comercial website and corresponds to an estimation for 2019 average Portuguese loads, for BTN C (normal low voltage, residential) [21]. This publicly available data is a fifteen-minute average, based on the year-before loads. This data is published at unit scale and was scaled to fit the PV installed power in the microgrid. The resulting load profile is presented in Figure 9.

After some simulations, a response time window of 3-5 seconds is achieved with success allowing real time control to be possible. In each control cycle the commands are sent, all the variables read and registered. To proper evaluate the strategy application, the best suited key-performance indicators were calculated.

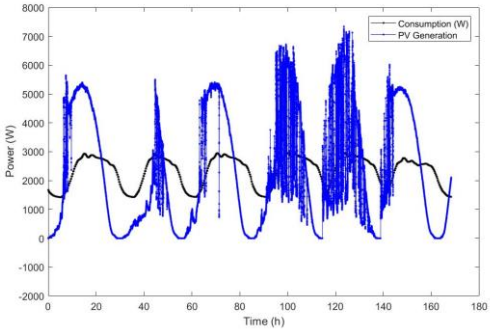

Figure 9: PV profile and load consumption.

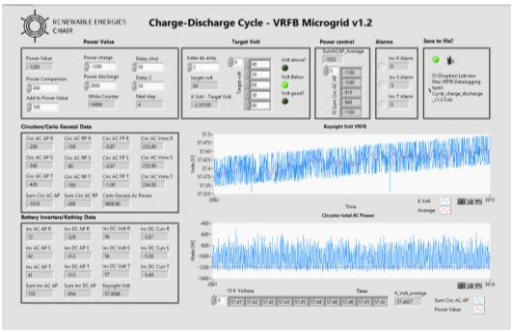

Figure 10: LabVIEW EMS implementation.

4.1 Key-performance indicators

- **Self-consumption ratio (SCR)** – Share of the PV generation consumed by the installation from the total of the PV energy generation.

$$SCR = \frac{E_{PVconsumed}}{E_{PVgenerated}} \quad (13)$$

Where, $E_{PVconsumed}$ is the PV energy generation consumed directly or indirectly (e.g. battery auxiliary consumption), and the $E_{PVgenerated}$ is the total PV energy generated by the PV system.

- **Self-sufficiency ratio (SSR)** – Share of the consumed PV energy generation in the total load consumption needs.

$$SSR = \frac{E_{PVconsumed}}{E_{Load}} = \frac{E_{Load} - E_{Grid}}{E_{Load}} \quad (14)$$

Where, E_{Load} is the total load consumption needs, and the E_{Grid} is the sum of the energy, which is injected and extracted from the network grid, in the overall strategy.

- **Grid-relief factor (GRF)** – The grid relief factor offers a measure of the total grid use in the overall load consumption needs.

$$GRF = \frac{E_{Load} - E_{Grid}}{E_{Load}} \quad (15)$$

- **Overall battery use (OBU)** – Share of energy of the power battery command in the overall energy consumption.

$$OBU = \frac{E_{Load} - (E_{charge} + E_{discharge})}{E_{Load}} \quad (16)$$

Where, E_{charge} is the total energy used to charge the battery, and the $E_{discharge}$ is the total energy used to discharge the battery, in the overall strategy.

- **Battery charge ratio (BCR)** – Total energy used to charge the battery, in the overall power battery commands sent to the battery.

$$BCR = \frac{E_{charge}}{E_{battery\_command}} \quad (17)$$

Where, $E_{battery\_command}$ is the total energy sent to charge and discharge the battery, in absolute values.

- **Energy from the grid (EG)** – Amount of energy extracted from the grid, considering the total grid use.

$$EG = \frac{E_{fromGrid}}{E_{Grid}} \quad (18)$$

Where, $E_{fromGrid}$ is the energy needed to extract from the grid to supply the energy needs, in the overall strategy.

- **From grid use (FGU)** – Amount of energy extracted from the grid in the overall energy needs.

$$FGU = \frac{E_{fromGrid}}{E_{Load}} \quad (19)$$

- **To grid use (TGU)** - Amount of energy injected into the grid in the overall energy needs.

$$TGU = \frac{E_{toGrid}}{E_{Load}} \quad (20)$$

Where, E_{toGrid} is the energy sent to the grid.

- **From battery use (FBU)** – Amount of energy extracted from the battery in the overall energy needs.

$$FBU = \frac{E_{fromBattery}}{E_{Load}} \quad (21)$$

Where, $E_{fromBattery}$ is the energy used to discharge from the battery.

- **To battery use (TBU)** – Amount of energy sent to the battery in the overall energy needs.

$$TBU = \frac{E_{toBattery}}{E_{Load}} \quad (22)$$

Where, $E_{toBattery}$ is the energy used to charge the battery.

4.2 EMS results evaluation

Regarding the overall EMS evaluation, the key-performance indicators obtained for this test are presented in Table V. One of the most important parameters for the battery control is the SOC at each point for the EMS to run accordingly. Figure 11, below shown, presents the obtained SOC evolution during the test timeframe, and Figure 12 represents the power exchanged with the battery and the power exchanged with the grid, over the experiment.

Table V: Resulting model Key Performance Indicators, over the 6 days of implementation.

Parameter	[%]
Self-consumption ratio (SCR)	67.02
Self-sufficiency ratio (SSR)	64.66
Grid-relief factor (GRF)	15.71
Overall battery use (OBU)	52.02
Battery Charge Ratio (BCR)	52.26
Energy from the grid (EG)	70.65
From grid use (FGU)	11.10
To grid use (TGU)	4.612
From battery use (FBU)	26.72
To battery use (TBU)	25.29

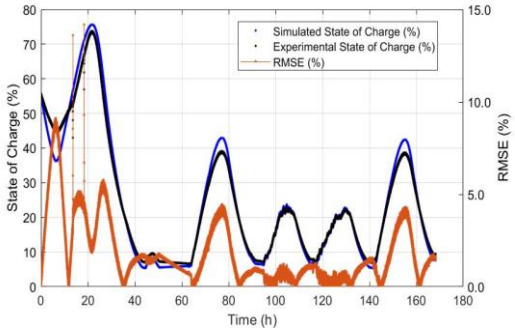

Figure 11: SOC of the VRFB along the EMS test period.

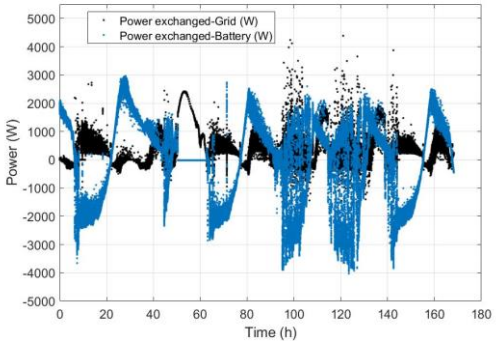

Figure 12: Power exchanged with the battery and the power exchanged with the grid, in the test period.

4.3 Results discussion

The equivalent electric circuit model of the VRFB has generated low error results for the key parameters (stack voltage, terminal voltage and terminal current), with increased computational simplicity and efficiency, as shown in the Figure 8 and Table IV. It accounts for the major VRB issues including thermal effects, transients, and dynamic SOC. The model seems to be suited for long term operation with lower computational effort, being validated by the presented results.

One of the problems in the battery characterization tests was the malfunctioning of the stack current sensor. This issue was already addressed and ongoing work on the model will also fine-tune this model parameter, lowering even further the error results presented here.

The validation of this model for the VRFB with experimental data in real operating conditions and at full scale, allowed to validate an equivalent electric circuit model requiring less computational resources, and implementing it within a microgrid EMS.
This EMS was tested and the resulting KPIs are consistent with good performance of the overall goal of self-consumption maximization. It resulted in values of SCR and SSR of 67% and 65% (respectively). TBU and FBU, indicators related to battery usage achieved 25% and 27%, to and from battery use respectively, over all the energy flow in the microgrid. With this strategy, a value of GRF of around 16% points to good results, given the PV generation with heavy intermittency due to clouds (Figure 9).
The simulated SOC presented low error (Figure 11), pointing to good model performance, thus validating it. Even though it is not an important simulation parameter for real control, since VRFB technology allows to measure this quantity in real time of battery operation, this is an important result for validation of the developed model.
The overall results obtained, point to a good approximation of the key parameters by the developed model and a good performance of the energy management strategy, reaching a self-consumption rate of 67%, even with very cloudy days.
The way of operating, control and test the battery are crucial aspects to achieve a good match among the simulation model and the real-time response. The developed control was made to achieve the best key-performance indicators and respecting the general operating limits of the battery.

5 CONCLUSIONS

Literature lacks optimal VRFB modelling, including ancillaries and power electronics solutions, modelling the electric, chemical and fluid-dynamic parameters according to the electric input and output power requirements. The fact that the VRFB has an online SOC real-time measurement, based on the reference stack voltage, allows a more precise control to be made, regarding other storage technologies, increasing its lifetime and reliability.
The presented results validate the developed simplified VRFB model and its implementation within a EMS was fully concluded achieving good final KPIs.
Implementing lower computational effort models allows the development of more intelligent energy management strategies, taking into account the optimization of internal battery model operating parameters. Implementing this EMS with fast response times (control loop under 3-5s) enable to deal with rapid intermittency or fast power ramps due to the load characteristics to be supplied.
In this work we chose to work with the simplest model with the highest accuracy, and the obtained results are as expected. The aim of the model is to be used in energy management strategies, and the results validate this assumption. Future work can include fine-tuning of internal model parameters and inclusion in other EMS or even EMS for hybrid battery systems.

6 ACKNOWLEDGEMENTS

The authors would like to thank the support of this work, developed under the European GRECO project, financed by 2020 Horizon under the grant agreement no. 787289. This work was also supported by the PhD. Scholarship (author Ana Foles) of FCT – Fundação para a Ciência e Tecnologia –, Portugal, with the reference SFRH/BD/147087/2019.

7 REFERENCES

[1] IRENA, *Innovation landscape for a renewable-powered future: Solutions to integrate variable renewables*. 2019.
[2] "redT energy storage." [Online]. Available: http://www.redtenergy.com.au/.
[3] M. Guarnieri, P. Mattavelli, G. Petrone, and G. Spagnuolo, "Vanadium Redox Flow Batteries," no. december 2016, pp. 20–31, 1932.
[4] P. Alotto, M. Guarnieri, and F. Moro, "Redox fl ow batteries for the storage of renewable energy : A review," vol. 29, pp. 325–335, 2014.
[5] R. D'Agostino, L. Baumann, A. Damiano, and E. Boggasch, "A Vanadium-Redox-Flow-Battery Model for Evaluation of Distributed Storage Implementation in Residential Energy Systems," *IEEE Trans. Energy Convers.*, vol. 30, no. 2, pp. 421–430, 2015.
[6] B. Chakrabarti *et al.*, "Modelling of redox flow battery electrode processes at a range of length scales: a review," *Sustain. Energy Fuels*, 2020.
[7] J. Chahwan, C. Abbey, and G. Joos, "VRB Modelling for the Study of Output Terminal Voltages , Internal Losses and Performance," pp. 387–392, 2007.
[8] T. A. Nguyen, X. Qiu, J. David, G. Ii, M. L. Crow, and A. C. Elmore, "Performance Characterization for Photovoltaic-Vanadium Redox Battery Microgrid Systems," vol. 5, no. 4, pp. 1379–1388, 2014.
[9] X. Qiu, T. A. Nguyen, J. D. Guggenberger, M. L. Crow, and A. C. Elmore, "A field validated model of a vanadium redox flow battery for microgrids," *IEEE Trans. Smart Grid*, vol. 5, no. 4, pp. 1592–1601, 2014.
[10] M. R. Mohamed, H. Ahmad, M. N. A. Seman, S. Razali, and M. S. Najib, "Electrical circuit model of a vanadium redox flow battery using extended Kalman filter," *J. Power Sources*, vol. 239, pp. 284–293, 2013.
[11] V. Viswanathan *et al.*, "Cost and performance model for redox fl ow batteries," *J. Power Sources*, vol. 247, pp. 1040–1051, 2014.
[12] A. Bhattacharjee and H. Saha, "Design and experimental validation of a generalised electrical equivalent model of Vanadium Redox Flow Battery for interfacing with renewable energy sources," *J. Energy Storage*, vol. 13, pp. 220–232, 2017.
[13] "MathWorks." [Online]. Available: https://www.mathworks.com/products/matlab.html.
[14] W. Paper, "Executive summary."
[15] EASE, "Flow Battery."
[16] R. Amirante, E. Cassone, E. Distaso, and P. Tamburrano, "Overview on recent developments in energy storage : Mechanical , electrochemical and hydrogen technologies,"

Energy Convers. Manag., vol. 132, pp. 372–387, 2017.

[17] H. Lopes, R. Garde, G. Fulli, W. Kling, and J. Pecas, "Characterisation of electrical energy storage technologies," *Energy*, vol. 53, pp. 288–298, 2013.

[18] G. L. Kyriakopoulos and G. Arabatzis, "Electrical energy storage systems in electricity generation : Energy policies , innovative technologies , and regulatory regimes," *Renew. Sustain. Energy Rev.*, vol. 56, pp. 1044–1067, 2016.

[19] X. Luo, J. Wang, M. Dooner, and J. Clarke, "Overview of current development in electrical energy storage technologies and the application potential in power system operation q," *Appl. Energy*, vol. 137, pp. 511–536, 2015.

[20] L. Fialho, T. Fartaria, L. Narvarte, and M. C. Pereira, "Implementation and validation of a self-consumption maximization energy management strategy in a Vanadium Redox Flow BIPV demonstrator," *Energies*, vol. 9, no. 7, 2016.

[21] EDP Distribuição, "Atualização dos perfis de consumo , de produção e de autoconsumo para o ano de 2018 Documento Metodológico (artigo 272 . º do Regulamento de Relações Comerciais)," 2018.